# HEAVY FLAVOR PRODUCTION AT LHCB IN LHC RUN I AND RUN II

Patrick Spradlin

University of Glasgow Particle Physics

LPNHE Seminar
19 March 2015, Paris, France

# ME

**1997** B.S. Physics with honors, California Institute of Technology (Caltech)

- Research with BaBar and the San Onofre Neutrino Oscillation Experiment.

**1997-2000** Aerospace engineer; simulation and software development.
**2000-2005** Ph.D. Physics, University of California, Santa Cruz

- Thesis: Measurements of the branching fraction, CP asymmetry, and isospin asymmetry of $B^0 \to K^{*0}\gamma$ and a search for the decays $B \to \rho\gamma$ and $B^0 \to \omega\gamma$ at BaBar.
- Medical applications of silicon strip detectors.

**2006-2011** Post Doctoral Research Assistant, University of Oxford

- Research at LHCb and CLEO-c,
- Founded and developed LHCb's Charm Physics Program.

**2011-present** Post Doctoral Research Assistant, University of Glasgow

- Research at LHCb,

# ME AT LHCb (2006-present)

Coordination and leadership,

- Coordinator of the first CP Working Group for Charm Physics, 2010-2011
- Coordinator of the Open Charm Production Task Force, 2010-2013
- Coordinator of the Charm Working Group for Production and Spectroscopy, 2011-present
- Chair of the Early 2015 Measurements Task Force, 2014-present.

Research highlights

- Search for $\Xi_{cc}^{+}$, JHEP 1312 (2013) 090,
- Search for direct CP violation in $D^0 \to h^- h^+$, Phys.Lett. B723 (2013) 33–43,
- Amplitude analysis of $D^0 \to K^+ K^- \pi^+ \pi^-$ at CLEO, Phys.Rev. D85 (2012) 122002.
- Prompt open charm hadron production in proton-proton collisions at $\sqrt{s} = 7\,\mathrm{TeV}$, Nucl.Phys. B871 (2013) 1–20,

Service

- Lead developer for the first implementation of LHCb's inclusive *b*-hadron (topological) trigger (2009-2010),
- Lead developer/coordinator/liaison for charm triggering,
- 20-40 Shift Leader and RICH piquet shifts per year since 2009.

# Shift Leader

# RICH PIQUET

# Outline

# OUTLINE

1. LHCb at the LHC
2. PRODUCTION MEASUREMENTS
3. CHARM HADRON PRODUCTION CROSS-SECTIONS
4. SELECTED ADDITIONAL PRODUCTION MEASUREMENTS
5. LHC RUN II

# LARGE HADRON COLLIDER

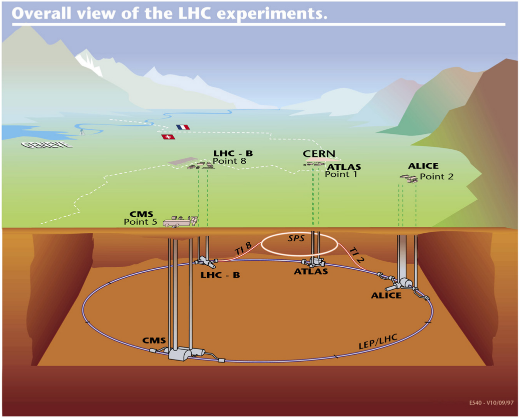

# FORWARD ACCEPTANCE

Forward acceptance $2 < \eta < 5$.

Takes advantage of the predominant forward production of heavy flavored hadrons.

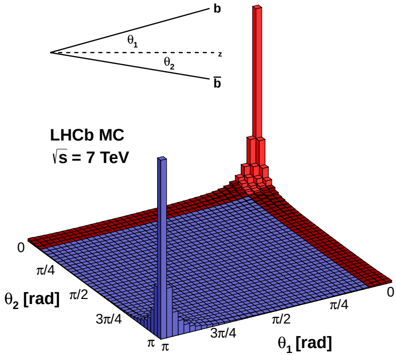


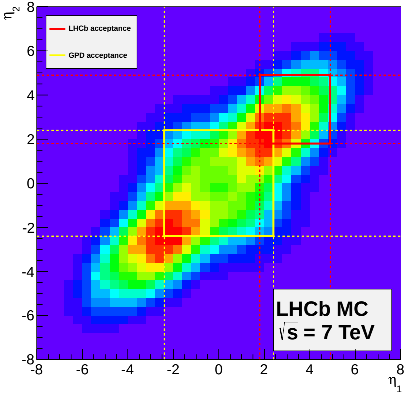


Pseudorapidity range unique among the LHC detectors.

Complementary to the GPDs.

# LHCb

LHCb: a forward-arm spectrometer at the LHC

Optimized for heavy flavor physics in *pp* collisions.

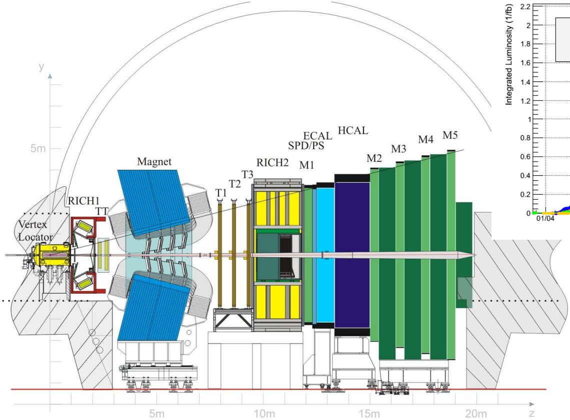


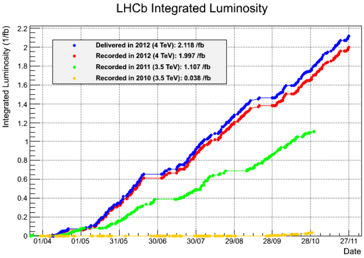


Data collection:

2010 38 $\text{pb}^{-1}$ $\sqrt{s} = 7\,\text{TeV}$,

2011 1.1 $\text{fb}^{-1}$ $\sqrt{s} = 7\,\text{TeV}$,

2012 2.0 $\text{fb}^{-1}$ $\sqrt{s} = 8\,\text{TeV}$.

# OUTLINE

# HEAVY FLAVOR PRODUCTION

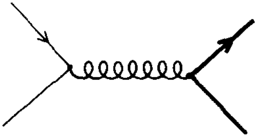

Production measurements of heavy flavor hadrons can be vital to improved understanding of QCD,

- Test precise cross-section predictions,
- Provide empirical fragmentation functions,
- Probe proton structure.

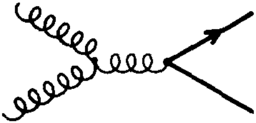

Necessary for MC generator tuning,

- Simulation inputs to precision flavor physics measurements,
- Long term program planning,
- New experiment design.

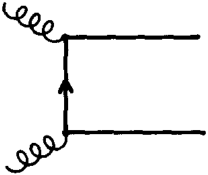

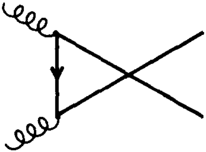

Standard Model backgrounds for New Physics searches,

- Absolute rates of SM processes must be known precisely.

# HEAVY PRODUCTION AND PROTON STRUCTURE

Heavy flavor forward production in LHC proton-proton collisions primarily through gluon-gluon fusion.

LHCb flavor production measurements cover a partonic momentum fraction $x$ complementary to the HERA DIS data,

- HERA: $10^{-4} < x \lesssim 10^{-1}$,
- LHCb: $5 \times 10^{-6} < x \lesssim 10^{-4}$.

Inclusion of LHCb data should improve precision of gluon PDFs at small $x$,

- Implications for lepton flux calculations in atmospheric showers.

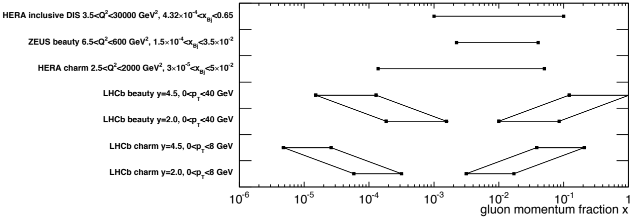


PROSA Collaboration, arXiv:1503.04581 [hep-ph].

# PROSA PDF FITS

PROSA collaboration incorporates LHCb production measurements into proton PDF fits.

Two approaches

- Fit absolute measured cross-sections, $\frac{d^2\sigma}{dp_T dy}$,
- Fit normalized cross-sections, $\frac{d\sigma}{dy} / \frac{d\sigma}{dy_0}$.

Significant improvement in precision at small $x$ and small $Q^2$.

Much smaller theory uncertainties in fit to normalized values,

- Absolute normalization subject to large uncertainties estimated by pQCD scale variation,
- Rapidity shape is largely scale invariant.

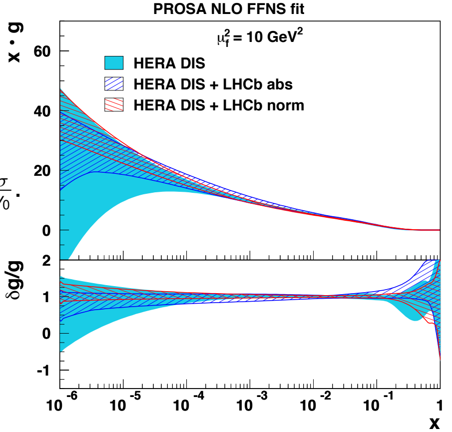


PROSA Collaboration, arXiv:1503.04581 [hep-ph].

# INTRINSIC CHARM IN PROTONS

Intrinsic charm/beauty are hypothetical $c\bar{c}$ or $b\bar{b}$ contributions to the proton beyond the 'sea'.

Several potential models have been explored in theory, including five-quark $uudc\bar{c}$ states and $D^0(u\bar{c})\Lambda_c^+(udc)$ quasi-two-body bound states.

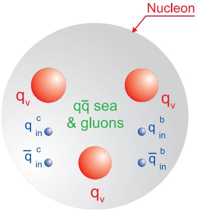


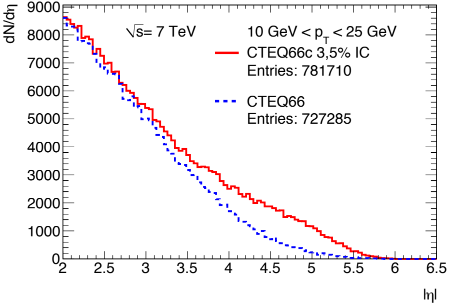


Europhys.Lett. 99 (2012) 21002 Fig. 9. Predicted $pp \to (D^0 + \bar{D}^0)X$ at $\sqrt{s} = 7\,\mathrm{TeV}$ and $10 \leq p_\mathrm{T} \leq 25\,\mathrm{GeV}/c$.

Evidence for intrinsic heavy flavor can manifest in production spectra.

Enhances forward production,

- Up to a factor of 3–10 for forward $\Lambda_b^0$ or $\Lambda_c^+$ production,
- Large enhancements in charmed meson production in ranges accessible to LHCb.

# GENERATOR TUNING

Monte Carlo simulations of proton-proton collisions are vital tools in experimental particle physics,

- Detector design and response,
- Control and analysis software validation,
- Estimation of measurement efficiencies.

All generators have tunable parameters

- Allows better matching to observables,
- Production measurements are the key ingredient.

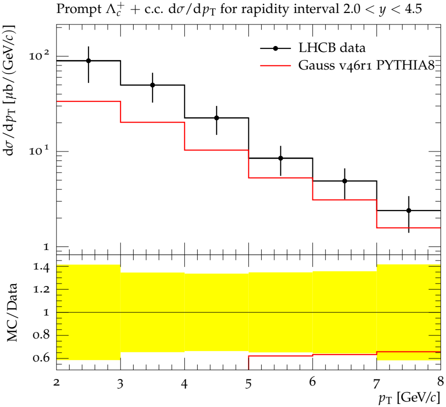


Rivet analysis of $\Lambda_c^+$ production in the LHCb tune of PYTHIA8.

Toolkits like Rivet and Professor facilitate tuning, providing an interface between generator output and measured distributions.

# Outline

# OPEN CHARM PRODUCTION CROSS-SECTIONS

Differential production cross-sections of open charm hadrons ($H_c$),

$$\frac{\mathrm{d}\sigma_i(H_c)}{\mathrm{d}p_\mathrm{T}} = \frac{1}{\Delta p_\mathrm{T}} \cdot \frac{N_i(H_c \to f + \text{c.c.})}{\varepsilon_{i,\mathrm{tot}}(H_c \to f) \cdot \mathcal{B}(H_c \to f) \cdot \mathcal{L}_\mathrm{int}}$$

In bins of $p_\mathrm{T}$ and $y$ as measured in the $pp$ CM frame

- Eight $1\,\mathrm{GeV}/c$ $p_\mathrm{T}$ bins in the range $0 < p_\mathrm{T} < 8\,\mathrm{GeV}/c$,
- Five 0.5 unit $y$ bins in $2 < y < 4.5$.
- * $\Lambda_c^+$ sample size allows only 1-D binning.

Samples of five hadrons in decays to favored decay modes to hadronic final states,

- $D^0 \to K^-\pi^+$
- $D^{*+} \to \pi^+ D^0(K^-\pi^+)$
- $D^+ \to K^-\pi^+\pi^+$
- $D_s^+ \to \phi(K^-K^+)\pi^+$
- $\Lambda_c^+ \to p^+K^-\pi^+$

Two additional less powerful modes analyzed as independent checks,

- $D^0 \to K^-\pi^+\pi^-\pi^+$
- $D^+ \to \phi(K^-K^+)\pi^+$

# CHARM IN HADRONIC COLLISIONS

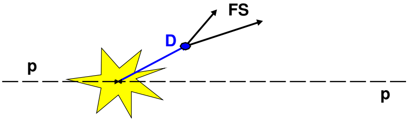


Prompt production

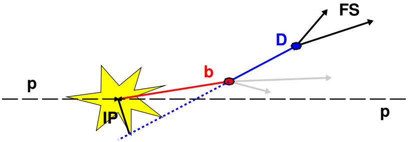


$b$ decays ($B \to D^{(*)} X$)

Two major sources of charm:

- Prompt: Produced at primary interaction,
  - Direct production,
  - Feed-down from higher resonances.
- Secondary: Produced in the decay of a $b$-hadron.

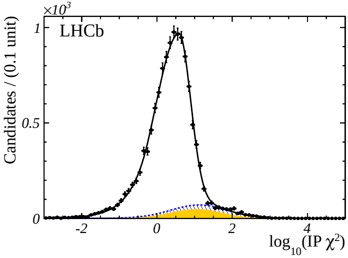


Isolate the prompt contribution,

- Fits to impact parameter (IP) $\chi^2$ distribution of the reconstructed $H_c$,
- No attempt to separate the two prompt production mechanisms.

# MEASUREMENT COMPONENTS

Published measurements with 15 $\text{nb}^{-1}$ of data collected in 2010.

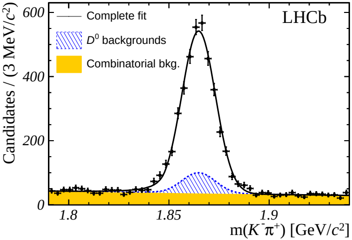


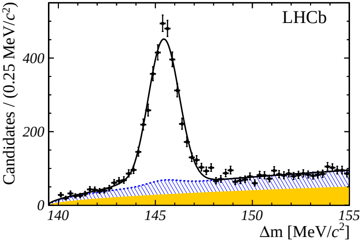


Prompt yield in each bin determined with 2D fit to mass and $\log_{10}(IP\chi^2)$.

Except $D^{*+}$, which requires 3D fit to mass, $\Delta m$, and $\log_{10}(IP\chi^2)$.

- $\Delta m \equiv m[\pi^+(K^-\pi^+)_D] - m(K^-\pi^+)$
- Separates $D^0$ + random pion backgrounds.

Efficiencies factorized into 4 components

$$\varepsilon_{i,\text{tot}} = \varepsilon_{i,\text{acc}} \cdot \varepsilon_{i,\text{trig|acc}} \cdot \varepsilon_{i,\text{sel|trig}} \cdot \varepsilon_{i,\text{pid|sel}}$$

- $\varepsilon_{i,\text{acc}}$ determined from MC studies,
- $\varepsilon_{i,\text{trig|acc}}$ uniform for this data set,
- $\varepsilon_{i,\text{sel|trig}}$ estimated with signal MC,
- $\varepsilon_{i,\text{pid|sel}}$ measured in data with independent PID calibration samples.

# DIFFERENTIAL CROSS-SECTIONS: $D^0$ AND $D^+$

NUCL.PHYS. B871 (2013) 1-20

**$\mathrm{d}\sigma/\mathrm{d}p_{\mathrm{T}}$ compared to predictions from FONLL and GMVFNS**

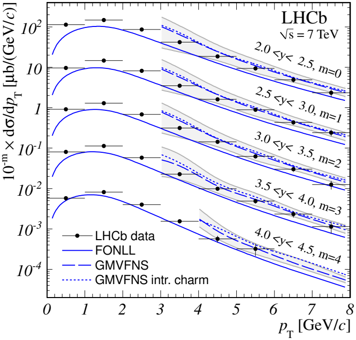


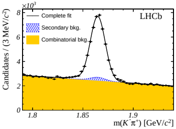


$D^0$ from $D^0 \to K^-\pi^+$

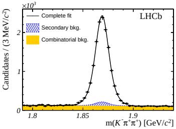


$D^+$ from $D^+ \to K^-\pi^+\pi^+$

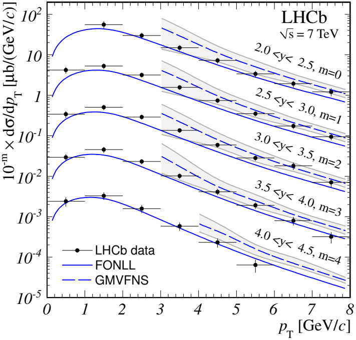


FONLL: Fixed-Order-Next-to-Leading-Logarithm, JHEP 1210 (2012) 137
GMVFNS: Generalized Mass Variable Flavour Number Scheme, Eur.Phys.J.C72 (2012) 2082

# DIFFERENTIAL CROSS-SECTIONS: $D_s^+$ AND $D^{*+}$

NUCL.PHYS. B871 (2013) 1-20

**$\mathrm{d}\sigma/\mathrm{d}p_\mathrm{T}$ compared to predictions from FONLL and GMVFNS**

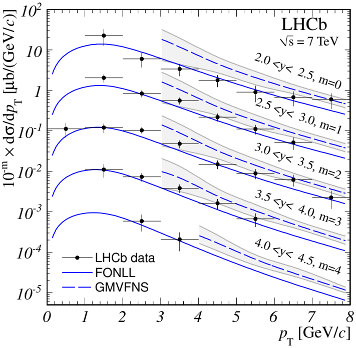


$D^{*+}$ from $D^{*+} \to D^0\pi^+$

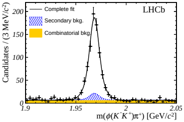


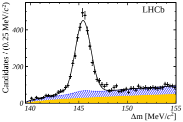


$D_s^+$ from $D_s^+ \to \phi(K^-K^+)\pi^+$

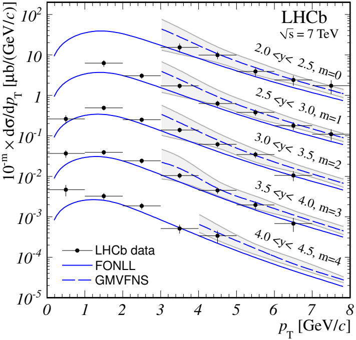


FONLL: Fixed-Order-Next-to-Leading-Logarithm, JHEP 1210 (2012) 137

GMVFNS: Generalized Mass Variable Flavour Number Scheme, Eur.Phys.J.C72 (2012) 2082

# DIFFERENTIAL CROSS-SECTIONS: $\Lambda_c^+ \to p^+ K^- \pi^+$

NUCL.PHYS. B871 (2013) 1-20

$d\sigma/dp_T$ compared to predictions from GMVFNS

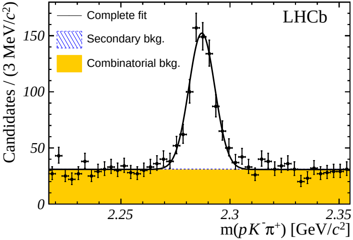


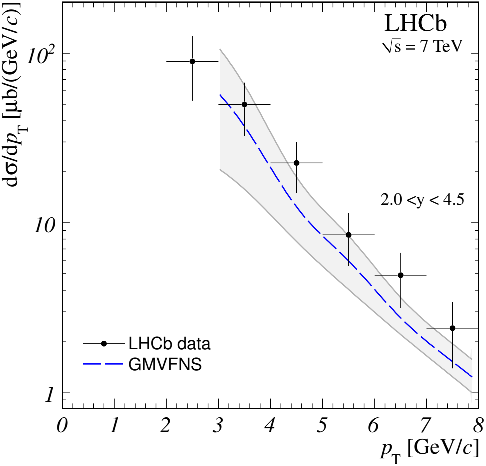

# INTEGRATED CROSS-SECTIONS

Integrated cross-sections over a common kinematic range for

- Determinations of cross-section ratios,
- Estimate of the total $c\bar{c}$ cross-section.

Integrate cross-sections over $p_{\mathrm{T}} < 8\,\mathrm{GeV}/c$ and $2 < y < 4.5$

- Sum all bins with $< 50\%$ total uncertainty,
- Extrapolate to full region with factors derived from MC.

| | Extrapolation factor, $f$ | Cross-section ($\mu$b) $\sigma \pm \mathrm{stat} \pm \mathrm{syst} \pm f$ |
|---|---|---|
| $D^0$ | $1.003 \pm 0.001$ | $1661 \pm 16 \pm 128 \pm 2$ |
| $D^+$ | $1.067 \pm 0.013$ | $645 \pm 11 \pm 72 \pm 8$ |
| $D^{*+}$ | $1.340 \pm 0.037$ | $677 \pm 26 \pm 77 \pm 19$ |
| $D_s^+$ | $1.330 \pm 0.056$ | $197 \pm 14 \pm 26 \pm 8$ |
| $\Lambda_c^+$ | $1.311 \pm 0.077$ | $233 \pm 26 \pm 71 \pm 14$ |

# CORRELATED UNCERTAINTIES

Three types of systematic uncertainties when combining results

1. Mode-correlated bin-correlated uncertainties (lumi and tracking),
2. Mode-uncorrelated bin-correlated uncertainties (BF and global corrections),
3. Uncorrelated uncertainties (PID, MC stat, *etc.*).

**Correlation matrix among results**

| | $\sigma(D^0)$ | $\sigma(D^+)$ | $\sigma(D^{*+})$ | $\sigma(D_s^+)$ |
|---|---|---|---|---|
| $\sigma(D^0) = 1661 \pm 129\,\mu b$ | | | | |
| $\sigma(D^+) = 645 \pm 74\,\mu b$ | 0.76 | | | |
| $\sigma(D^{*+}) = 677 \pm 83\,\mu b$ | 0.77 | 0.73 | | |
| $\sigma(D_s^+) = 197 \pm 31\,\mu b$ | 0.55 | 0.52 | 0.53 | |
| $\sigma(\Lambda_c^+) = 233 \pm 77\,\mu b$ | 0.26 | 0.25 | 0.25 | 0.18 |

# RATIOS AND TOTAL CROSS-SECTION

Cross-section ratios determined from integrated cross-sections

| | $\sigma(D^0)$ | $\sigma(D^+)$ | $\sigma(D^{*+})$ | $\sigma(D_s^+)$ |
|---|---|---|---|---|
| $\sigma(D^+)$ | $0.389 \pm 0.029$ | | | |
| $\sigma(D^{*+})$ | $0.407 \pm 0.033$ | $1.049 \pm 0.092$ | | |
| $\sigma(D_s^+)$ | $0.119 \pm 0.016$ | $0.305 \pm 0.042$ | $0.291 \pm 0.041$ | |
| $\sigma(\Lambda_c^+)$ | $0.140 \pm 0.045$ | $0.361 \pm 0.116$ | $0.344 \pm 0.111$ | $1.183 \pm 0.402$ |

Using form factor values $f(c \to H_c)$ from PDG, we get 5 estimates of the total $c\overline{c}$ cross-section in $p_{\mathrm{T}} < 8\,\mathrm{GeV}/c$, $2 < y < 4.5$. The average:

$$\sigma(c\overline{c})_{p_{\mathrm{T}}<8\,\mathrm{GeV}/c,\,2.0<y<4.5} = 1419 \pm 12\,(\mathrm{stat}) \pm 116\,(\mathrm{syst}) \pm 65\,(\mathrm{frag})\;\mu\mathrm{b}.$$

# OUTLINE

# FROM INCLUSIVE $b\overline{b}$ TO HADRON CROSS-SECTIONS

Two LHCb measurements of the inclusive $b\overline{b}$ production cross-section for $pp$ $\sqrt{s} = 7\,\mathrm{TeV}$ (extrapolated to $4\pi$)

- Using $b \to D\mu\nu X$ with $14.9\,\mathrm{nb}^{-1}$ (Phys. Lett. B694 (2010) 209-216)
  $\sigma(pp \to b\overline{b}X) = 284 \pm 20 \pm 49\,\mu\mathrm{b}$
- Using detached $J/\psi$ with $5.2\,\mathrm{pb}^{-1}$ (Eur. Phys. J. C 71 (2011) 1645)
  $\sigma(pp \to b\overline{b}X) = 288 \pm 4 \pm 48\,\mu\mathrm{b}$

Related to production cross-sections of specific $b$-hadron species by fragmentation functions

- Here we use $f_q \equiv \mathcal{B}(b \to B_q)$, $f_{\Lambda_b^0} \equiv \mathcal{B}(b \to \Lambda_b^0)$,
- In principle, can depend on $\sqrt{s}$ and location in $b$ phase space.

Necessary for normalization of $B_s^0$ and $\Lambda_b^0$ branching ratio measurements at LHC

- Also useful for sensitivity and background studies.

Two measurements of fragmentation function ratios at LHCb.

# $\sigma(pp \to b\bar{b}X)$ WITH $b \to D^0 \mu\nu X$

PHYS.LETT. B694 (2010) 209-216

Analysis of $D^0(K^-\pi^+)\mu$ combinations in $14\,\mathrm{nb}^{-1}$ at $\sqrt{s} = 7\,\mathrm{TeV}$.

Separation of prompt $D^0$ and $D^0$ from $b$ with log of impact parameter of $D^0$ with respect to PV.

Differential cross-sections in 4 bins of $\eta$, where $\eta$ is determined by the displacement from the PV to the $D^0\ \mu^-$ vertex.

Converted to $\sigma(pp \to b\bar{b}X)$ with inclusive $\mathcal{B}(b \to D^0\mu^-\nu_\mu X)$.

Integrated over fiducial region $\sigma(pp \to H_b X, 2 < \eta < 6) = 75.3 \pm 5.4 \pm 13.0\,\mu\mathrm{b}$.

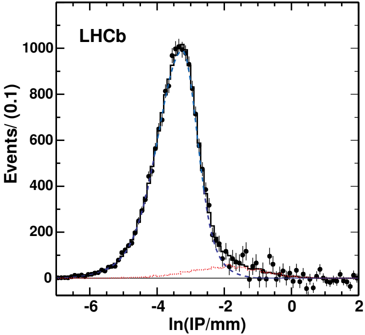


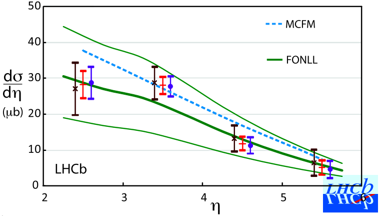

# $\sigma\, pp \to b\bar{b}X$ WITH $b \to J/\psi\, X$

EUR.PHYS.J. C71 (2011) 1645

Analysis of 565,000 $J/\psi \to \mu^+\mu^-$ in 5.2 $\text{pb}^{-1}$ at $\sqrt{s} = 7\,\text{TeV}$.

Separation of prompt $J/\psi$ and $J/\psi$ from $b$ with pseudo-proper time

$$t_z = \frac{(z_{J/\psi} - z_V)M_{J/\psi}}{p_z}$$

Double differential cross-sections in 14 bins of $p_\text{T}$ and 5 bins of $y$

$$\mathrm{d}^2\sigma(J/\psi \text{ from } b)/\mathrm{d}p_\text{T}\mathrm{d}y$$

Integrated over fiducial region

$$\sigma(J/\psi \text{ from } b, p_\text{T} < 14\,\text{GeV}, 2.0 < y < 4.5) = 1.14 \pm 0.01 \pm 0.16\,\mu\text{b}.$$

Converted to $\sigma(pp \to b\bar{b}X)$ with inclusive $\mathcal{B}(b \to J/\psi\, X)$.

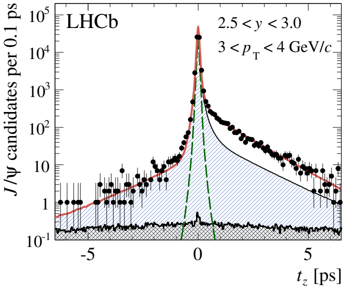


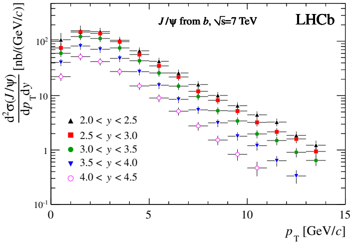

# $f_s/f_d$ WITH $B \to Dh$

PHYS. REV. LETT. 107 (2011) 211801 (35 $\text{pb}^{-1}$)

Three decay modes for two determinations of $f_s/f_d$:

$$B^0 \to D^- K^+, \qquad B^0 \to D^- \pi^+, \qquad B_s^0 \to D_s^- \pi^+.$$

Using theoretical expressions for the branching fractions, the ratio from $B_s^0 \to D_s^- \pi^+$ and $B^0 \to D^- K^+$ is

$$\frac{f_s}{f_d} = 0.971 \left|\frac{V_{us}}{V_{ud}}\right|^2 \left(\frac{f_K}{f_\pi}\right)^2 \frac{\tau_{B^0}}{\tau_{B_s^0}} \frac{1}{\mathcal{N}_a \mathcal{N}_F} \left(\frac{\epsilon(D^- K^+)}{\epsilon(D_s^- \pi^+)} \frac{N(D_s^- \pi^+)}{N(D^- K^+)}\right)$$

and that from $B_s^0 \to D_s^- \pi^+$ and $B^0 \to D^- \pi^+$ is

$$\frac{f_s}{f_d} = 0.982 \frac{\tau_{B^0}}{\tau_{B_s^0}} \frac{1}{\mathcal{N}_a \mathcal{N}_F \mathcal{N}_E} \left(\frac{\epsilon(D^- \pi^+)}{\epsilon(D_s^- \pi^+)} \frac{N(D_s^- \pi^+)}{N(D^- \pi^+)}\right)$$

$N(X)$ and $\epsilon(X)$ are the experimental yields and efficiencies, $\mathcal{N}_a$ parameterizes nonfactorizable SU(3)-breaking, $\mathcal{N}_F$ is the ratio of form factors, and $\mathcal{N}_E$ accounts for the $W$-exchange diagram in $B^0 \to D^- \pi^+$.

# $f_s/f_d$ WITH $B \to Dh$

PHYS. REV. LETT. 107 (2011) 211801

Result from $B_s^0 \to D_s^- \pi^+$ and $B^0 \to D^- K^+$

$$\frac{f_s}{f_d} = (0.310 \pm 0.030(\text{stat}) \pm 0.021(\text{syst}))\frac{1}{\mathcal{N}_a\mathcal{N}_F}$$

and that from $B_s^0 \to D_s^- \pi^+$ and $B^0 \to D^- \pi^+$ is

$$\frac{f_s}{f_d} = (0.307 \pm 0.017(\text{stat}) \pm 0.023(\text{syst}))\frac{1}{\mathcal{N}_a\mathcal{N}_F\mathcal{N}_E}$$

Combining the two with substituted theory parameters

$$\frac{f_s}{f_d} = 0.253 \pm 0.017(\text{stat}) \pm 0.017(\text{syst}) \pm 0.020(\text{theor})$$

$B_s^0 \to D_s^- \pi^+$

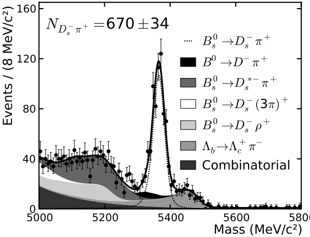


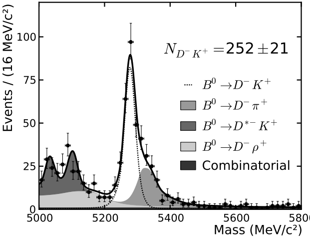


$B^0 \to D^- K^+$

# $f_{s(\Lambda_b^0)}/(f_u + f_d)$ WITH SEMILEPTONIC DECAYS

PHYS. REV. D 85 (2012) 032008 (3 $\text{pb}^{-1}$)

Attempt to reduce theoretical input by analyzing the abundances of the products of semileptonic *b*-hadron decays.

Six inclusive final states

- $\Lambda_c^+ \mu^+ \nu X$ and $D^0 p \mu^+ \nu X$ to determine abundance of $\Lambda_b^0$, $n_{\text{corr}}(\Lambda_b^0 \to D\mu)$,
- $D_s^- \mu^+ \nu X$ and $\bar{D}^0 K^- \mu^+ \nu X$ to determine abundance of $B_s^0$, $n_{\text{corr}}(B_s^0 \to D\mu)$,
- $\bar{D}^0 \mu^+ \nu X$ and $D^- \mu^+ \nu X$ with corrections from the other final states to determine the combined abundance of $B^0$ and $B^+$, $n_{\text{corr}}(B^0 \to D\mu) + n_{\text{corr}}(B^+ \to D\mu)$.

*b*-hadron semileptonic decays separated from prompt *D* production with characteristic distribution of *D* impact parameter.

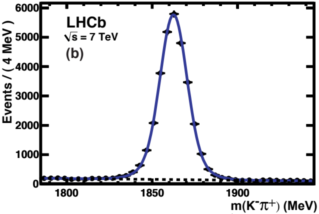


Mass $m(K^- \pi^+)$

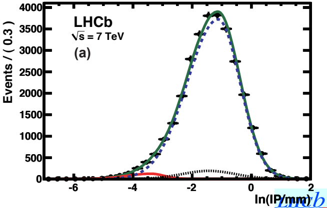


$\log(IP/\text{mm})$

# $f_{s(\Lambda_b^0)}/(f_u + f_d)$ WITH SEMILEPTONIC DECAYS

PHYS. REV. D 85 (2012) 032008

From these,

$$\frac{f_s}{f_u + f_d} = \frac{n_{\mathrm{corr}}(B_s^0 \to D\mu)}{n_{\mathrm{corr}}(B^0 \to D\mu) + n_{\mathrm{corr}}(B^+ \to D\mu)} \frac{\tau_{B^+} + \tau_{B^0}}{2\tau_{B_s^0}}$$

and

$$\frac{f_{\Lambda_b^0}}{f_u + f_d} = \frac{n_{\mathrm{corr}}(\Lambda_b^0 \to D\mu)}{n_{\mathrm{corr}}(B^0 \to D\mu) + n_{\mathrm{corr}}(B^+ \to D\mu)} \frac{\tau_{B^+} + \tau_{B^0}}{2\tau_{\Lambda_b^0}}(1 - \xi)$$

where the factor $\xi$ accounts for the chromomagnetic correction that affects $b$ mesons but not $b$ baryons.

Analyzed as a function of $D\mu$ $p_{\mathrm{T}}$ in two bins of $D\mu$ $\eta$ to investigate variations in phase space.

# $f_s/(f_u + f_d)$ WITH SEMILEPTONIC DECAYS

PHYS. REV. D 85 (2012) 032008

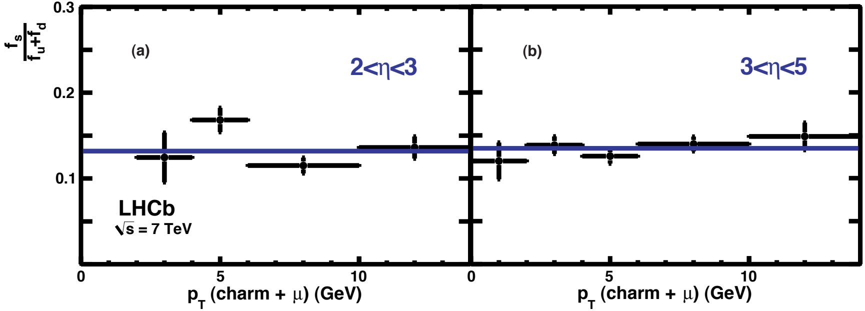


No sign of $p_{\mathrm{T}}$ dependence for $f_s/f_u + f_d$

Constant fit to all data gives

$$\frac{f_s}{f_u + f_d} = 0.134 \pm 0.004^{+0.011}_{-0.010}$$

# $f_{\Lambda_b^0}/(f_u + f_d)$ WITH SEMILEPTONIC DECAYS

PHYS. REV. D 85 (2012) 032008

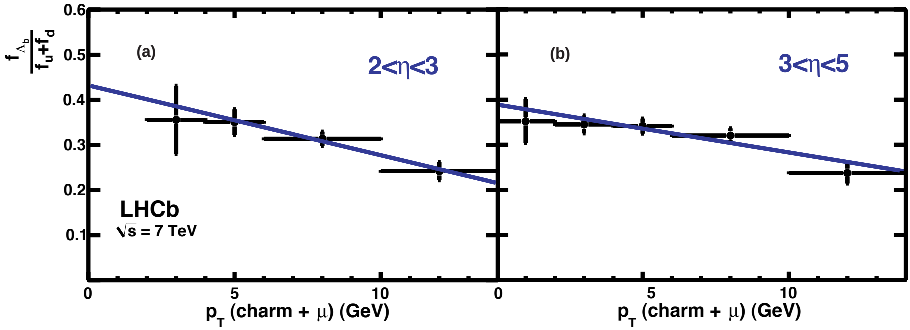


Apparent $p_{\mathrm{T}}$ dependence for $f_{\Lambda_b^0}/f_u + f_d$.

Expressing the result as a best-fit linear function of $p_{\mathrm{T}}$:

$$\left[f_{\Lambda_b^0}/(f_u + f_d)\right](p_{\mathrm{T}}) = a \times [1 - b \times p_{\mathrm{T}}],$$

$$a = 0.404 \pm 0.017(\mathrm{stat}) \pm 0.027(\mathrm{syst}) \pm 0.105(\mathrm{BF}) \quad (1)$$

$$b = 0.031 \pm 0.004 \pm 0.003\,\mathrm{GeV}^{-1}$$

# $B^{\pm}$ PRODUCTION CROSS-SECTION
JHEP 04 (2012) 039

Measured in the mode $B^{\pm} \to J/\psi K^{\pm}$

- $\sim$9100 signal events in $35\,\text{pb}^{-1}$ $\sqrt{s} = 7\,\text{TeV}$ data,

Total cross-section and $\mathrm{d}\sigma/\mathrm{d}p_{\mathrm{T}}$

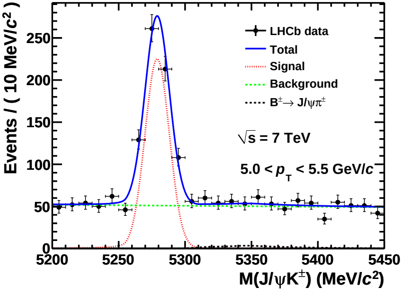


Mass distribution for bin $5 < p_{\mathrm{T}} < 5.5\,\mathrm{GeV}/c$

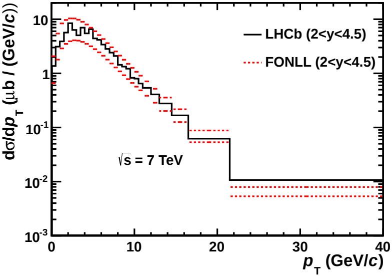


Differential $\mathrm{d}\sigma/\mathrm{d}p_{\mathrm{T}}$ compared to FONLL predictions (JHEP 03 (2001) 006),

- $f_{\bar{b}\to B^{+}} = (40.1 \pm 1.3)\%$.

$\sigma(pp \to B^{\pm}X) = 41.4 \pm 1.5(\text{stat}) \pm 3.1(\text{syst})\,\mu\text{b}$ for $0 < p_{\mathrm{T}} < 40\,\mathrm{GeV}/c$, $2 < y < 4.5$.

# Outline

# LHC Run II is fast approaching!

In early 2013, LHC Run I concluded and operations entered the machine's first Long Shutdown (LS1).

- Maintenance, refurbishment, safety system improvements, *etc.*

Shutdown activities are now concluding, beam commissioning activities are starting.

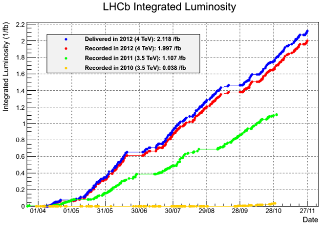


LHCb data collection in Run I.

LHC Run II will feature several improvements to extend its physics reach, including

- Increased instantaneous luminosity
  - Spacing between successive proton bunches halved,
  
  $\Rightarrow$ More proton bunches per beam.
- Greater *pp* collision energy, $\sqrt{s} = 13\,\mathrm{TeV}$
  - Up from $8\,\mathrm{TeV}$ in 2012.

A new energy regime in which to study heavy flavor production!

# Staged restart

Return to normal operations at the new configuration will begin in late spring 2015 and will go through several stages, including

1. Collisions with new energy, $\sqrt{s} = 13\,\mathrm{TeV}$, but old bunch spacing ($50\,\mathrm{ns}$),
2. Collisions with new energy, $\sqrt{s} = 13\,\mathrm{TeV}$, but new bunch spacing ($25\,\mathrm{ns}$).

The $13\,\mathrm{TeV}$, $50\,\mathrm{ns}$ operation will be only a few weeks,

- Safely push to $25\,\mathrm{ns}$ as soon as practical.

While the precision decay physics program of LHCb will need the much larger integrated luminosity of the $25\,\mathrm{ns}$ operation, production measurements can be made with significantly less data,

- The collaboration has designated the $13\,\mathrm{TeV}$, $50\,\mathrm{ns}$ data specifically for production measurements!

# Draft schedule

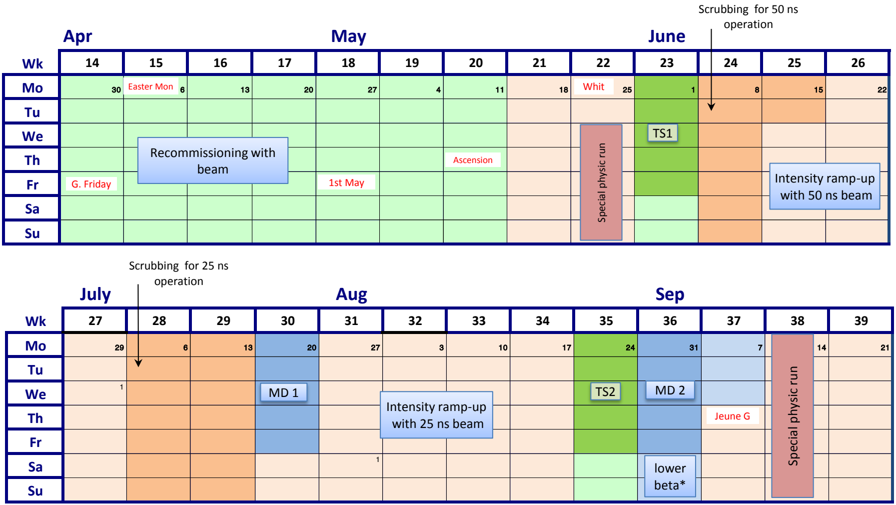


Normal data collection continues through October; heavy ion collisions begins in mid November.

# Early 2015 Measurements Task Force

LHCb created the Early 2015 Measurements Task Force to coordinate analysis and calibration activities to ensure the rapid exploitation of the LHCb data to be taken in 2015, specifically for production measurements at the new collision energy.

The task force coordinates most aspects of the operational and analysis planning for the data collected at $\sqrt{s} = 13\,\mathrm{TeV}$,

- Collision conditions,
- Triggers optimized for production measurements,
- Data processing,
- Luminosity calibration,
- Measurements of PID and tracking efficiency,
- Physics measurements!.

# PRODUCTION MEASUREMENTS

Preliminary estimates for 13 TeV, 50 ns data collection point to an integrated luminosity of 30–40 $\mathrm{pb}^{-1}$,

- Equivalent in size to the 2010 data set,
- Excellent for the production measurements described in this seminar.

We are customizing the data collection and trigger conditions for a broad set of production measurements,

- Soft QCD and strangeness production,
  - Forward energy flow,
  - Charged particle multiplicity,
  - Total inelastic cross-section,
  - $K^0_S$ production cross-section,
  - $\phi$ production cross-section,
  - $\Lambda$ production and $V^0$ production ratios.
- Production of $c\bar{c}$ and $b\bar{b}$ bound states ($J/\psi$, $\Upsilon(nS)$, *etc.*)
- Measurements of $B$ cross-sections and production fractions,
- Open charm production cross-sections.
- . . . and more!

# SUMMARY

Heavy flavor production measurements are crucial to our understanding of the Standard Model.

Precise understanding of heavy flavor production is also necessary for continued searches for New Physics.

LHCb's forward design allows it to probe a unique region of heavy flavor production.

LHCb has published several high-impact measurements of heavy flavor production at $\sqrt{s} = 7\,\mathrm{TeV}$ and $8\,\mathrm{TeV}$, and are poised to continue the program into the new energy regime.

The LHCb Early 2015 Measurements Task Force will execute data collection and prepare analysis well enough to lead to new and exciting results for the summer conferences.